JOURNAL OF MATERIALS SCIENCE 19 (1984) 2606–2614

Stress relaxation behaviour of some aromatic compounds and their alloys with linear polyethylene

B. HAGSTRÖM, J. KUBÁT
Chalmers University of Technology, Department of Polymeric Materials, S-412 96 Gothenburg, Sweden

The paper reports on stress relaxation measurements on piperonal, camphor and dimethyl terephthalate (DMTP), and on alloys of high density polyethylene (HDPE) with camphor, DMTP and thymol. The pure compounds were measured in compression, the HDPE-alloys in tension. The course of the relaxation curves is in certain cases complicated by recrystallization of the low molecular weight substances and also by sublimation stresses. When these effects are accounted for, the previously found general relationship between the slope F of the curves, $(d\sigma/d \ln t)_{max}$, and the initial effective stress, σ_0^*, i.e.

$$F = (0.1 \pm 0.01)\, \sigma_0^*$$

is confirmed. The results thus extend the validity of this structure-independent relation to low molecular weight aromatic substances and their alloys with a crystalline polymer.

1. Introduction

Solid state flow, as stress relaxation and creep, has been studied in detail for a long time in materials like metals, polymers, and ceramics [1–5]. Simple organic substances and alloys of polymers with such substances have, however, attracted only very limited interest. This article reports on measurements of stress relaxation in piperonal, dimethyl terephthalate (DMTP) and camphor, and in alloys of high molecular weight linear polyethylene (HMWPE) with camphor, DMTP and thymol. The pure compounds were tested in compression, the alloys in tension. The results are discussed in terms of relaxation models currently used for polymers and metals.

A stress relaxation curve usually has a sigmoid shape when plotted in a stress–log (time) diagram. This is true for polymers as well as for metals. The linear region of the curves, coinciding with the inflection region, covers a few decades of time, while the entire relaxation process (as approximated by a straight line) extends over about 4 decades. The slope of the linear region, defined as $F = (-d\sigma/d \ln t)_{max}$, where σ denotes the stress and t the time, has been found to be related to the initial stress (σ_0) of the relaxation experiments as [6]:

$$F = (0.1 \pm 0.01)(\sigma_0 - \sigma_i) \quad (1)$$

Here σ_i is the internal stress, which corresponds to the stress level asymptotically reached after a long time [6]. The stress difference $(\sigma_0 - \sigma_i)$ is referred to as the initial effective stress, σ_0^*.

The purpose of this work was to investigate whether Equation 1, known to be obeyed by a large variety of solids [7], is also valid for some simple molecular substances and their alloys with a semicrystalline polymer (HMWPE). We found that the stress relaxation behaviour of camphor and piperonal was more complex than normally observed, the main difference being the occurrence of two inflection regions in the relaxation curves. The first inflection appeared to be associated with structural changes (recrystallization), while the second constituted the normally observed process complying with Equation 1. The first inflection was suppressed by repeating the relaxation on the same sample without unloading, the validity of Equation 1 thus being recovered.

The stress relaxation behaviour of alloys of

0022–2461/84 $03.00 + .12 © *1984 Chapman and Hall Ltd.*

linear polyethylene with camphor, thymol and DMTP had the normal appearance, giving fair agreement with Equation 1. In some cases, sublimation effects influenced the shape of the final stage of the relaxation curves. This effect was especially pronounced with thymol and camphor.

2. Theoretical background

The flow behaviour of metals, and recently also of polymers, is often interpreted in terms of the theory of stress-aided thermal activation [6, 8], which for stress relaxation can be written as

$$\dot{\sigma} = d\sigma/dt = -A' \exp(-\Delta G/kT) \quad (2)$$

with σ denoting the (time-dependent) stress, ΔG the activation energy, kT the thermal energy, and A' a constant. If it is assumed that the activation energy decreases linearly with increasing effective stress (σ^*), Equation 2 yields

$$\dot{\sigma} = -A \exp(v\sigma^*/kT) \quad (3)$$

where v is the activation volume and A the pre-exponential factor. Equation 3 describes the linear part of the relaxation curves (at higher relative stresses/shorter times) called the exponential law region. The maximum stress rate, F, is related to the activation volume as [6]:

$$F = kT/v \quad (4)$$

Using Equation 1, one can write the exponential law as:

$$\dot{\sigma} = -A \exp(\alpha\sigma^*/\sigma_0^*) \quad (5)$$

where $\alpha \approx 10$ for a large number of different materials. Note that σ_0^* refers to the total stress dissipated during the experiments.

At lower relative stresses (σ/σ_0), that is longer times, the stress dependence of the rate $\dot{\sigma}$ is described by a power law. Details pertaining to the analysis of stress relaxation curves can be found in [6]. In the present case, only the exponential part of the relaxation curves is commented upon.

3. Experimental details

3.1. Materials

The low molecular weight (LMW) organic substances used in this study were analytical grades of piperonal (T_m 39° C), dimethyl terephthalate (DMTP) (T_m 141° C), camphor (T_m 178° C), and thymol (T_m 50° C). With the exception of thymol, they were investigated in their pure forms, while camphor, DMTP and thymol were also used as alloys with high molecular weight linear polyethylene (HMWPE).

The pure LMW substances were compression-moulded at room temperature (500 MPa, 1 min) into cylindrical billets with a length of 30 mm, and a diameter of 8 mm.

The HMWPE-grade used was DMDS 2215 (in powder form), Unifos Kemi AB, density 0.953 g cm^{-3}, $\bar{M}_w$ 286 000, $\bar{M}_n$ 22 000 (GPC-values).

The alloys were prepared by compression moulding 1 mm thick sheets from mixtures of HMWPE (powder) and the finely ground LMW substances (0.5 MPa, 200° C, 60 min, cooling rate 10° C min^{-1}). From these sheets tensile testing bars with the dimensions 50 mm × 5 mm × 1 mm were cut.

The systems camphor/HMWPE and DMTP/HMWPE are of the eutectic type, while thymol acts as a low melting diluent. All these systems, except 50% camphor in HMWPE containing primary-grown camphor crystals, are characterized by highly dispersed structures. The corresponding phase diagram and structural details will be given in a forthcoming publication [9].

The pure LMW compounds and the different alloys were not annealed because of sublimation damage to the samples.

3.2. Relaxation measurements

The relaxation experiments with the LMW compounds were performed on cylindrical samples in compression at room temperature (22 ± 0.2° C) using a stress relaxometer similar to that described in [10]. The maximum strain was 0.5%, and the strain rate 1.7×10^{-3} sec^{-1}.

The HMWPE-alloys (tensile test bars) were measured at 24 ± 0.1° C using a tensile stress relaxometer described elsewhere [10]. The stress–time data were recorded with a microcomputer. The maximum strain was 1%, the strain rate 1.25×10^{-2} sec^{-1}.

4. Results

4.1. Piperonal

Stress relaxation curves obtained with piperonal are shown in Fig. 1 for initial stresses (σ_0) varying between 0.24 and 1.85 MPa. Evidently, the initially applied stress has a strong influence on the shape of these curves. A low initial stress results in a rapid relaxation, while an increase in σ_0 yields a reduction in relaxation rate when the curves are

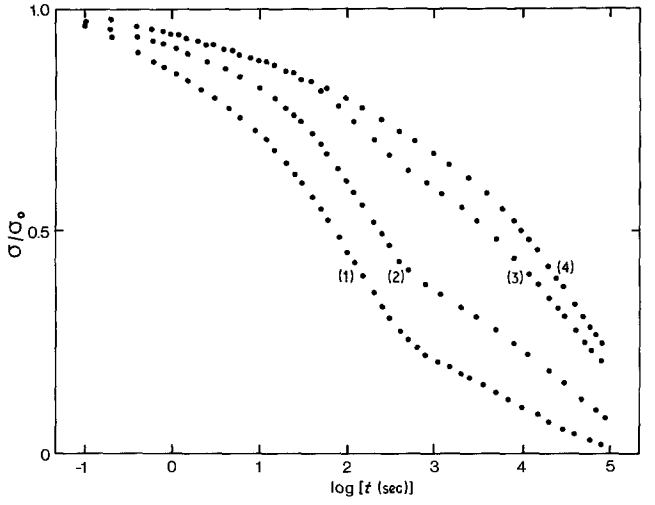

Figure 1 Representative stress relaxation curves for piperonal. Increasing numbers refer to increasing initial stresses, 0.24, 0.37, 0.97, and 1.85 MPa, respectively.

plotted in a normalized (σ/σ_0) stress–log (time) diagram. The maximum slope F/σ_0 decreases as σ_0 increases, and the curves exhibit two inflection regions. This will be further discussed below.

A convenient way of studying the relaxation kinetics is to plot the stress rate, $-\mathrm{d}(\sigma/\sigma_0)/\mathrm{d}\ln t$, against the normalized stress σ/σ_0. This method has been proposed by Li [11] for assessing internal stresses in metals, and it has also been applied to polymers [12]. Li-plots for piperonal at different initial stresses are shown in Fig. 2. It is evident that under the conditions used here the behaviour of piperonal is governed by two processes. An attempt was made to separate the two peaks in the Li-plot, as indicated in Fig. 2. In this way an effective initial stress for each process can be isolated.

In Fig. 3 the effective initial stresses for the first, σ_{01}^*, and the second, σ_{02}^*, process are shown against the total initial stress σ_0. There seems to be approximately a one-to-one correspondence between σ_{02}^* and σ_0, the $\sigma_{02}^*(\sigma_0)$-line being shifted by an approximately constant amount along the σ_0-axis from the origin. This also indicates that below $\sigma_0 \approx 0.15$ MPa the second inflection is barely detectable, the first mechanism dominating the process. Fig. 3 further shows an approximately linear relationship between σ_{01}^* and σ_0, although the slope of the straight line is significantly less than one. The values of σ_{01}^* for the higher σ_0 values are somewhat uncertain due to the difficulty in separating the first peak at higher initial stresses (cf. Fig. 2).

In Fig. 4 the maximum slope of the second inflection (F_2) is plotted against σ_{02}^*, yielding a straight line with a slope of 0.12, in fair agreement

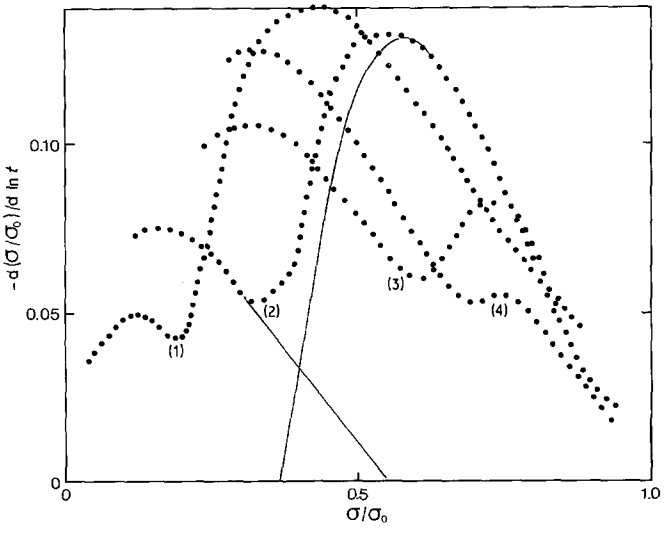

Figure 2 Li-plots [$-\mathrm{d}(\sigma/\sigma_0)/\mathrm{d}\ln t$ against σ/σ_0] for the stress relaxation curves shown in Fig. 1. The figure also illustrates the method used for separating the two peaks.

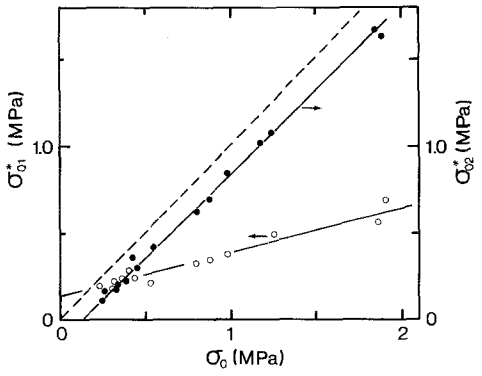

Figure 3 Initial effective stresses for the first (σ^*_{01}) and the second (σ^*_{02}) process against total initial stress (σ_0) for piperonal.

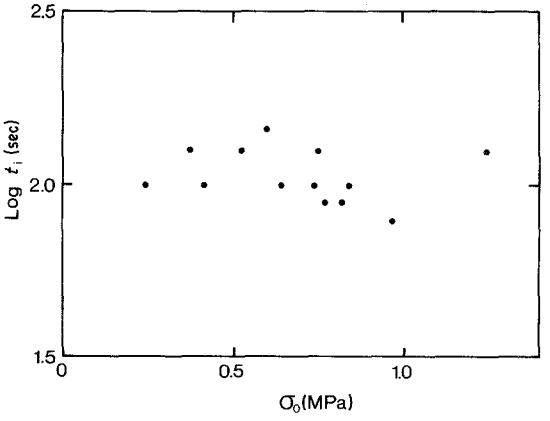

Figure 5 The time t_i corresponding to the maximum slope of the first inflection F_1 against the total initial stress σ_0 for piperonal.

with Equation 1. For the first inflection the corresponding ratio, i.e. F_1/σ^*_{01}, is significantly higher, *c.* 0.20.

In an attempt to characterize the first mechanism further, the time t_i corresponding to the maximum slope of the first mechanism in the σ/σ_0–log t curves is plotted against the initial stress σ_0 (Fig. 5). As can be seen, t_i is almost independent of σ_0 ($t_i \approx 100$ sec).

If the first mechanism is due to some strain-induced transformation, it can be expected not to appear in a second stress relaxation experiment performed after the stress has relaxed to a low level (after a few days). Fig. 6 shows that this is, indeed, the case. The second experiment yields a normal curve with only one inflection. Second stress relaxation experiments performed according to this procedure produce a linear F–σ_0 dependence with the slope 0.12 in agreement with the result obtained for the second inflection of the first run as discussed above.

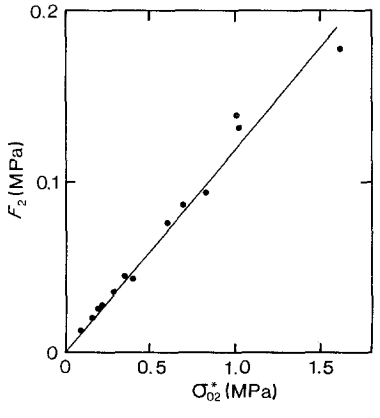

Figure 4 The maximum slope of the second inflection F_2 against σ^*_{02} for piperonal.

The intensity of the first inflection has been found to depend on the state of the material. For instance, with samples moulded from finely ground piperonal, the first inflection was very weak, the curves being dominated by the second mechanism with $F/\sigma_0 \approx 0.11$.

It should be noted that σ_0 for piperonal coincides with σ^*_0, since the internal stress is close to zero according to the Li-plots.

4.2. Camphor and dimethyl terephthalate

For camphor (Fig. 7) a double inflection similar to that observed for piperonal was recorded. This is evident from the Li-plot shown in Fig. 7. The time t_i, corresponding to the maximum slope of the first mechanism in the σ/σ_0–log t curves, was approximately the same (100 sec) as for piperonal. In this case, second stress relaxation did not completely suppress the first process, as shown in Fig. 7. The second measurements yielded $F/\sigma^*_0 \approx 0.10$, in good agreement with Equation 1.

The stress relaxation of DMTP had a normal appearance (Fig. 7). The ratio F/σ^*_0 was about 0.10, i.e., in agreement with Equation 1.

According to the Li-plots, there is no indication of significant internal stresses in camphor or DMTP.

4.3. Camphor/HMWPE

The stress relaxation behaviour of alloys of camphor and HMWPE is shown in Fig. 8, where typical curves normalized with respect to σ_0 are

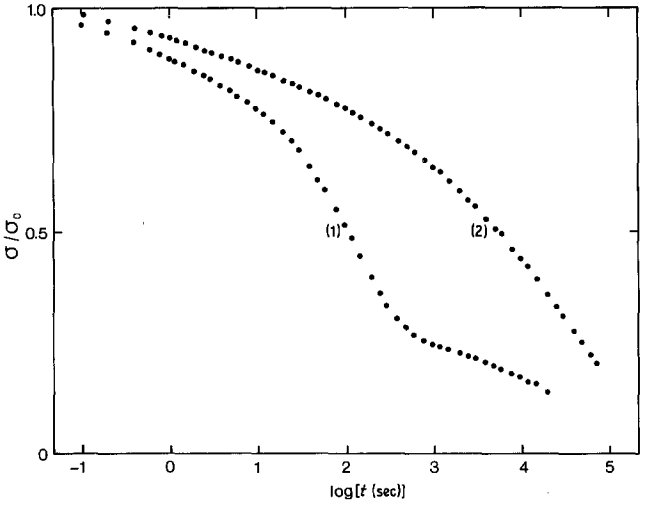

Figure 6 Stress relaxation curves for piperonal. 1. First run stress relaxation. 2. Second run stress relaxation without unloading the remaining stress from the first experiment. The initial stresses were 0.38 and 0.45 MPa, respectively.

reproduced along with the corresponding Li-plots. Neither the shape nor the position along the time axis was affected by the σ_0 level in the range of 1 to 7 MPa.

With regard to the influence of the camphor content, one notes a shift toward shorter times for the relaxation curves obtained with the alloyed samples, the half-times at $\sigma/\sigma_0 = 0.5$ being 120, 60, 40 and 80 sec for pure HMWPE, and for the alloys with 10, 30 and 50% camphor. It follows that there is an inversion in the shift at the eutectic point (*c.* 30% camphor).

A complicating factor is shrinkage stresses caused by a slow sublimation of the camphor phase during the relaxation measurement. Such stresses counteract the relaxation process. A qualitative illustration of this effect is given in Fig. 8. As can be seen, the shrinkage stresses increase with the camphor concentration. At 10%, the effect is negligible. The shrinkage curves were obtained in the relaxometer at low initial stresses (*c.* 0.01 MPa). In the Li-plots, shown in Fig. 8, this effect is reflected in the downward curvature of the final stage (50% camphor).

In Fig. 9, the slope F is plotted against σ_0, yielding straight lines. Again, the eutectic alloy has an extremal character, giving $F/\sigma_0 = 0.090$. The corresponding values for pure HMWPE and

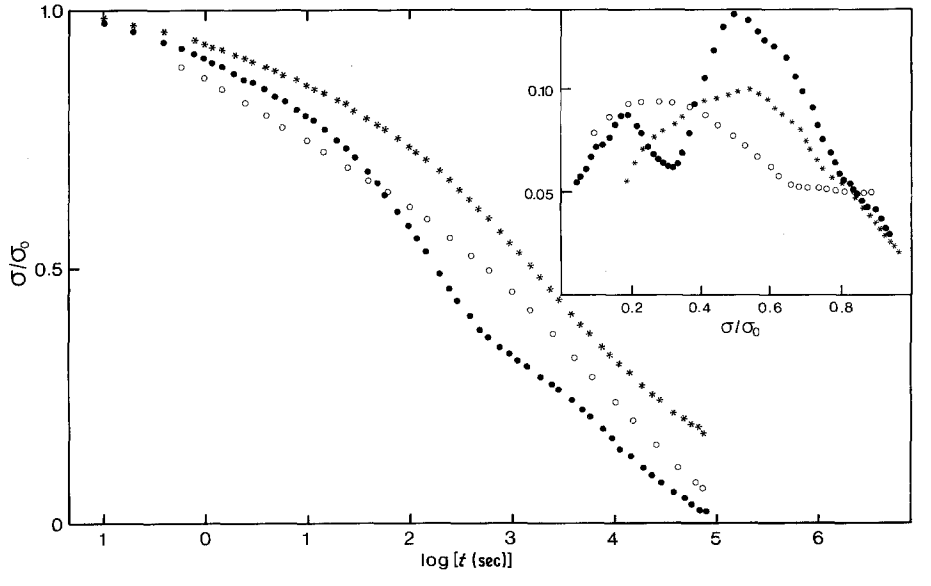

Figure 7 Stress relaxation curves and corresponding Li-plots for camphor, (•) first relaxation, (○) second relaxation and DTMP (*). The initial stresses were 0.48, 0.30 and 0.46 MPa, respectively.

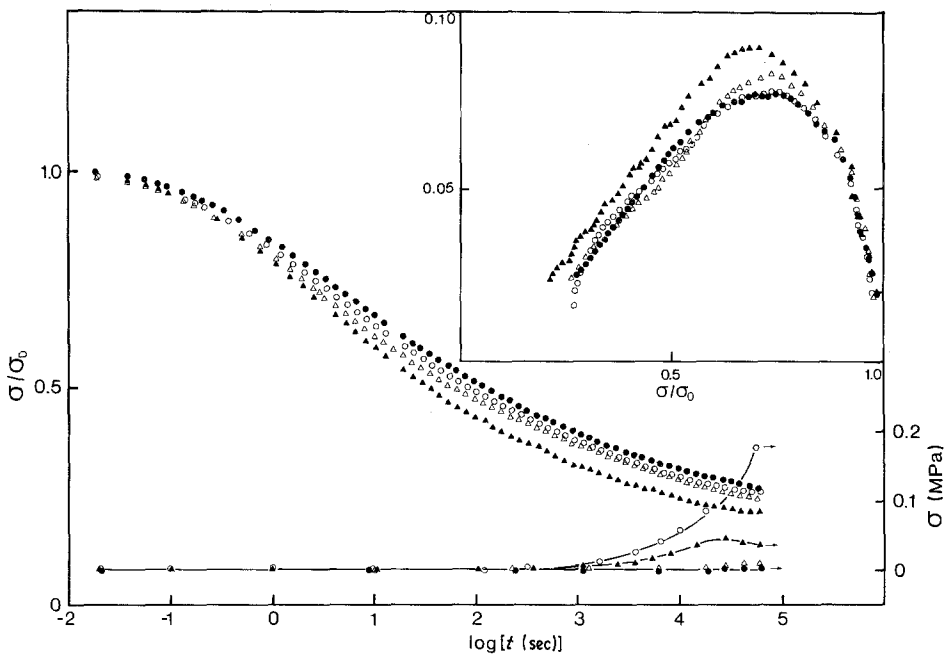

Figure 8 Stress relaxation curves and corresponding Li-plots for pure HMWPE (•) and alloys with 10% (△), 30% (▲), and 50% (○) camphor. The initial stresses were 5.1, 4.4, 5.3 and 3.5 MPa, respectively. Shrinkage stresses for the various alloys are also included.

alloys with 10 and 50% camphor are 0.077, 0.083 and 0.080, respectively. The intercepts of these lines with the σ_0-axis mark values close to zero of the permanent internal stress, σ_{ir} [12, 13].

The σ_i value determined by the σ_∞-level of the relaxation curves after sufficiently long measuring times allows the calculation of σ_0^* to check on the validity of Equation 1. However, the measurement of the equilibrium stress σ_∞ can hardly be employed in normal practice, due to the long measuring times involved. On the other hand, if it is assumed that a power law ($\dot{\sigma} \sim \sigma^n$) is valid in the entire low stress region, the σ_i-value can be determined from the intercept by the extrapolated linear portion of the Li-plot and the σ/σ_0-axis [12, 13]. In the present case, this procedure gives for F/σ_0^* the values 0.088, 0.090 and 0.098 for HMWPE and the alloys containing 10% and 30% camphor, respectively. For the 50%-alloy, this vaue was not measured, as the shape of the relaxation curves was distorted by sublimation stresses.

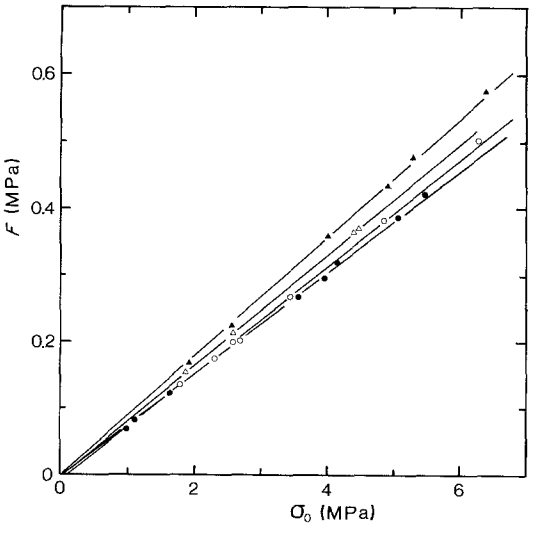

Figure 9 F against σ_0 for pure HMWPE and alloys with 10% (△), 30% (▲), and 50% (○) camphor.

4.4. Thymol/HMWPE

The stress relaxation behaviour of alloys of thymol and HMWPE is shown in Fig. 10, where some typical curves are reproduced. A plot of F against σ_0 is also included. The σ/σ_0–log t curves are shifted toward shorter times with increasing concentration of thymol. The half-times at $\sigma/\sigma_0 = 0.5$ are 120, 60 and 45 sec for HMWPE and the 10% and 30% alloys. The position along log t and the shape of the curves were not affected by the σ_0-value.

In this case, sublimation stresses also influenced

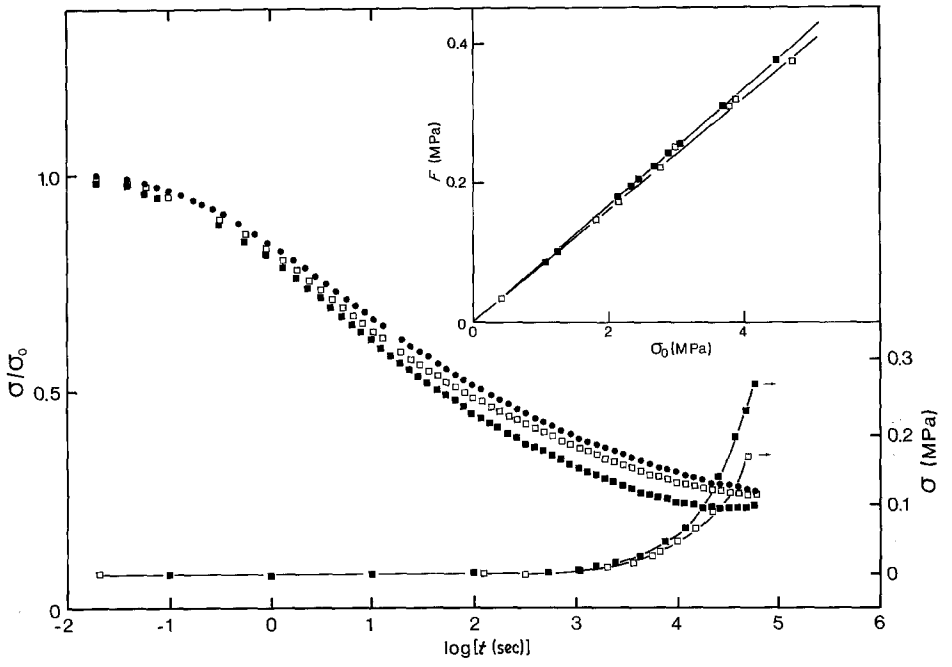

Figure 10 Stress relaxation curves for pure HMWPE and alloys with 10% (□), and 30% (■) thymol. The initial stresses were 5.1, 4.7 and 3.7 MPa, respectively. Also shown are F against σ_0, and shrinkage stresses for alloys with 10% and 30% thymol.

the final stage of the curves. A plot of these stresses against log t is included in Fig. 10. These values, which were determined in the relaxometer on samples at low σ_0-values (0.01 MPa), increase with thymol concentration. The effect appears to be more pronounced than in the camphor/HMWPE case; at small σ_0-values, it may reverse the direction of the final stage of the relaxation curves (cf. Fig. 10).

The F against σ_0 lines for the 10% and 30% alloys have the values 0.081 and 0.085, respectively. Calculating the σ_i-values by extrapolating the Li-plots yielded small positive values (about 3.5% of σ_0) for the 10%, and zero or negative values for the 30% alloy. These effects, probably due to sublimation, prevent a proper calculation of the correct value of the constant of Equation 1.

4.5. DMTP/HMWPE

A final illustration of the remarkable insensitivity of the relaxation process to changes in the composition of the relaxing solid is Fig. 11, which compares the behaviour of HMWPE with alloys containing 10% (eutectic) and 20% DMTP. The average half-time value of the 10% alloy is 80 sec, i.e. somewhat shorter than for the pure polymer and the 20% alloy. The slopes of the F against σ_0 plot were 0.091 and 0.084 for the 10 and 20% alloys, respectively.

The permanent internal stress, σ_{ir}, calculated from the intercept of the $F(\sigma_0)$-line with the σ_0-axis according to [13], was relatively large in this case, amounting to c. 0.5 MPa. On the other hand, the internal stress level σ_i, as obtained from the Li-plots, amounted to a few per cent of σ_0 only. Kubát *et al.* [12] have proposed that σ_i is the sum of σ_{ir} and σ_{id}, the latter quantity denoting the contribution to σ_i associated with the deformation of the sample in connection with the relaxation experiment. The discrepancy in the two σ_i-values found in the present case, i.e. σ_{ir} exceeding the total σ_i value obtained from the Li-plots, is probably due to the lack of validity of the power law ($\dot{\sigma} \sim \sigma^n$) in the entire low stress range. The σ_i-values calculated in this way may thus appear too low. No sublimation-induced shrinkage stresses were observed with the 10 and 20% DMTP alloys.

5. Discussion

The results of this study show that the course of the stress relaxation process in low molecular weight compounds may be complicated by several effects. One of them, the appearance of two

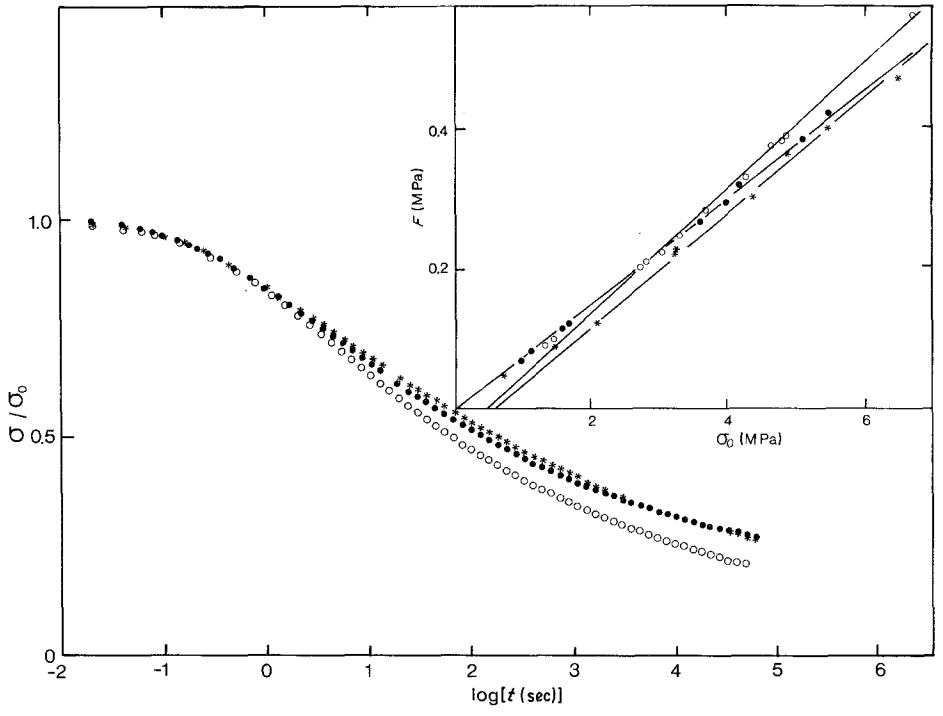

Figure 11 Stress relaxation curves and F against σ_0 for pure HMWPE (•), and alloys with 10% (○) and 20% DMTP (∗). The initial stresses were 5.1, 6.7 and 6.5 MPa, respectively.

inflection regions in the $\sigma(\log t)$ curves, has been tentatively associated with a strain-induced recrystallization phenomenon. In fact, wide-angle X-ray scattering diagrams of the samples showing this phenomenon provided direct evidence for this assumption being true. It was found that the orientation and size of individual grains could be changed significantly by the application of relatively low stresses. Recrystallization was especially pronounced in coarse-grained samples, which also showed the most pronounced irregularities of the relaxation behaviour. In samples prepared by compression moulding of finely ground material, only limited deviations from Equation 1 were found. Similar phenomena have been observed earlier with certain metals [14]. In some respects this situation resembles that encountered with elastomeric materials, where a distinction has to be made between the normal physical relaxation and flow processes due to chemical scission of the chains [15, 16].

Another complicating factor found in this investigation was the sublimation tendency of some of the compounds used, especially thymol and camphor. As shown in Figs. 8 and 10, this effect certainly brought about a distortion of the final portion of the $\sigma(\log t)$ curves. Even though sublimation does not affect the initial part of the relaxation curves from which the quantity F is determined, it influences the evaluation of σ_i entering the effective stress and thus Equation 1.

When the effects of recrystallization are eliminated, the results obtained support the validity of Equation 1, thus adding to its generality and independence of composition and structure. Indirectly, the results support the idea of a structure-independent co-operative mechanism responsible for the kinetics of the stress relaxation process in solids. In fact, a model has recently been constructed which yields the particular value of the constant in Equation 1 in terms of multiple elementary processes interacting in a way reminiscent of Bose–Einstein statistics [17, 18].

As the primary aim of this investigation was a check of the validity of Equation 1, only the exponential portion of the $\sigma(\log t)$ curves was analysed. The power law portion appearing in the final stage of the process has not been considered, partly due to the distortion brought about by the sublimation effect.

The results found with DMTP/HMWPE, where σ_{ir} was larger than the total σ_i-value obtained

from the Li-plot, indicate that deviations from the power law may in fact occur. Similar deviations have also been found recently with pure HDPE using a two-step relaxation technique [19]. The σ_i-values found above may thus be too low, which would point towards an even better agreement with Equation 1 for both the pure and alloyed materials. The consequences of the validity of Equation 1, for instance the apparent character of the volume of activation and of the entire concept of the hypothesis of the stress-aided thermal activation, have been discussed at length elsewhere [6]. The reader should also consult earlier reports on the significance of the two kinds of internal stress appearing in the above results, i.e. the permanent stress, σ_{ir}, evaluated from the $F(\sigma_0)$ plots, and the strain-induced internal stress, σ_{id} [12, 13].

References

1. J. GITTUS, "Creep, Viscoelasticity and Creep Fracture in Solids" (Applied Science Publishers Ltd., London, 1975).
2. F. GAROFALO, "Fundamentals of Creep-Rupture in Metals" (Macmillan Co., New York, 1965).
3. A. TOBOLSKY, "Properties and Structure of Polymers" (John Wiley & Sons, Inc., New York, 1960).
4. I. M. WARD, "Mechanical Properties of Solid Polymers" (Wiley, London, 1971).
5. L. E. NIELSEN, "Mechanical Properties of Polymers" (Reinhold, New York, 1962).
6. J. KUBÁT and M. RIGDAHL, *Phys. Status Solidi (a)* **35** (1976) 173.
7. J. KUBÁT, Thesis, Stockholm University, Stockholm (1965).
8. R. DE BATIST and A. CALLENS, *Phys. Status Solidi (a)* **21** (1974) 59.
9. B. HAGSTRÖM and J. KUBÁT, to be published.
10. J. KUBÁT, *Arkiv Fysik* **45** (1963) 493.
11. J. C. M. LI, *Canad. J. Phys.* **45** (1967) 493.
12. J. KUBÁT, M. RIGDAHL and R. SELDÉN, *J. Appl. Polym. Sci.* **20** (1976) 2799.
13. J. KUBÁT and M. RIGDAHL, *Int. J. Polym. Mater.* **3** (1975) 287.
14. J. KUBÁT, *Arkiv Fysik*, **28** (1965) 329.
15. M. ITO, *Polymer* **23** (1982) 1515.
16. G. M. BARTENEW, *Plaste und Kautschuk* **21** (1974) 499.
17. CH. HÖGFORS, J. KUBÁT and M. RIGDAHL, *Phys. Status Solidi (b)* **107** (1981) 147.
18. J. KUBÁT, *ibid.* **111** (1982) 599.
19. J. KUBÁT, L.-Å. NILSSON and M. RIGDAHL, *Mater. Sci. Eng.* in press.

Received 17 October
and accepted 3 November 1983